phys. stat. sol. (a) **85**, 349 (1984)

Subject classification: 1.1; 22.1.1

Department of Physics, Erevan State University[1]) *(a)*
and I. V. Kurchatov Institute of Atomic Energy, Moscow (b)

Six-Beam X-Ray Diffraction in Ge Single Crystals

By

P. A. BESIRGANYAN (a), R. TS. GABRIELYAN (a), V. G. KOHN (b),
and A. H. TONEYAN (a)

Results of an experimental and theoretical analysis are presented, concerning the six-beam $(220/242/044/\bar{2}24/\bar{2}02)$ diffraction of X-rays in thick perfect Ge crystals, under the conditions when a part of the diffracted beams is Bragg reflected. Three cases are considered, when one, three, or all five diffracted beams are Bragg reflected. It is shown theoretically that an enhancement of anomalous transmission for the Laue beams takes place in all these cases. Experimentally this effect is observed in the third case on the incident beam topogram, when the two-beam Borrmann effect corresponds to Bragg reflection and is more weakly revealed than in the Laue case. Experimentally as well as theoretically an unusual behaviour of the integral intensity for the (044) beam is observed, when the number of Bragg beams varied from one to five.

Представлены результаты экспериментальных и теоретических исследований шестиволновой $(220/242/044/\bar{2}24/\bar{2}02)$ дифракции рентгеновских лучей в толстых совершенных кристаллах германия в условиях, когда часть дифрагированных пучков отражается по Брэггу. Рассмотрены три случая, в которых по Брэггу отражается один, три и все пять дифрагированных пучков. Теоретически показано, что во всех рассмотренных сулчаях имеет место усиление аномального прохождения Лауэ-пучков. Экспериментально этот эффект обнаружен в третьем случае на топограмме прямого пучка, когда двухволновой эффект Бормана соответствует отражению по Брэггу и проявляется более слабо, чем в случае Лауэ. Как экспериментально, так и теоретически обнаружено необычное поведение интегральной интенсивности (044)-пучка при изменении числа Брэгг-пучков от одного до пяти.

1. Introduction

Six-beam X-ray scattering in perfect crystals represents one of the most interesting and relatively complex phenomena in solid-state physics. This scattering may be realized because of the high axial symmetry of the crystals, due to which certain reciprocal lattice points form hexads of vectors, representing polygons inscribed into a circle. In diamond, silicon, and germanium crystals, the simplest such case, namely $(220/242/044/\bar{2}24/\bar{2}02)$, has theoretically been considered for the first time in [1]. Subsequently the six-beam diffraction has been considered both theoretically and experimentally in [2 to 12], experiments being carried out on Ge crystals.

In all these works such a geometry of experiment has been considered when diffracted beams emerged from the crystals through the output surface, i.e. represented the Laue-type beams. Actually all the reflecting planes were assumed to be normal to the surface. The reason of this assumption apparently lies in the fact that it was for such a geometry in [1] that a strong enhancement of the anomalous transmission effect has been predicted, i.e. a decrease of the minimum interference absorption coefficient

[1]) Mravyan 1, 375049 Erevan 49, USSR.

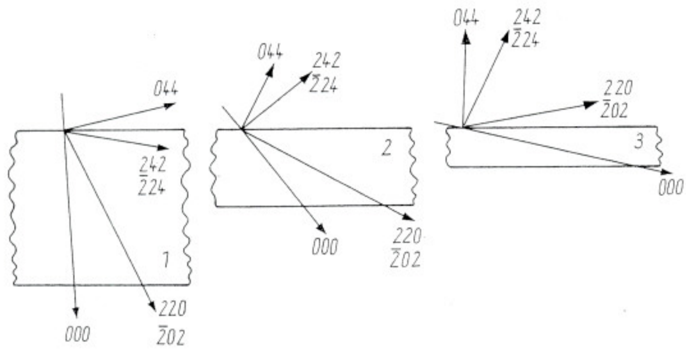

Fig. 1. Various diagrams of mixed Bragg-Laue geometry in the six-beam diffraction

(IAC) by a factor of several thousands for the exact multibeam direction of the incident plane wave [8]. In this case an analytical solution of the problem is also possible, which helps to get physical insight into the phenomenon.

Nevertheless, it is interesting to analyse the features of the six-beam X-ray diffraction for such an experimental set-up when some of the diffracted beams leave the crystal through the input surface, i.e. are Bragg reflected. Cutting the crystal surface at a certain angle α to a plane of reciprocal lattice vectors (H-plane) and normally to the scattering plane for the (044)-reflection (S-plane), one can realize the cases where one, three, or all five diffracted beams are Bragg reflected. In Fig. 1 beam path schemes for these cases are shown in their projection on the S-plane, where the incident and the (044)-diffracted beams lie.

From a practical viewpoint it is important to give an answer to the following question: how does the presence of Bragg-reflected beams influence the enhancement of anomalous transmission of Laue beams. In the two-beam Bragg scattering case the minimum IAC is known to decrease in a certain range of angles in the vicinity of the Bragg angle, as compared with the single-beam case, but not so strong as in the Laue case. Also of great interest is the character of the angular dependence of the intensity distribution both of Laue and Bragg reflected beams, particularly the "aufhellung" effect.

These are the problems considered in the present paper. We have found both experimentally and theoretically that the anomalous transmission enhancement effect takes place over a broad range of angles α, and that the symmetrical case ($\alpha = 0$) considered earlier is by no means optimum. Theoretical analysis has been carried out following the scheme described in [13], but in order to be able to calculate the Laue beam intensities for thick crystals we have developed the perturbation theory using a small parameter $\exp(-t/L_A)$, where t is the crystal thickness and L_A the absorption depth. The physical mechanism of the anomalous enhancement effect turned out to be the same as in the Laue case: the wave field for certain regions of the dispersion surface forms a two-dimensional standing wave in the H-plane, the nodes of which coincide with the atomic coordinates in that plane. The intensity distribution in the Bragg-reflected beams has a number of interesting features.

2. Experimental Observations

CuK_α and MoK_α radiation from a BSV-7 tube has been used in the experiments, having focus dimensions 0.1×0.1 mm². A plane-parallel plate of a dislocation-free Ge single crystal was placed at a distance of 250 cm from the source. In order to prevent intensity losses in air, a vacuum tube with beryllium windows has been placed between the source and the crystal. In order to obtain all the reflections simultaneously on the same film, the latter has been placed at a distance of a few centimeters from the sample. In a number of cases (when individual Bragg reflections were analysed) the film was placed at a distance of 2 to 3 m from the sample. The sample surface has been treated mechanically (lapped) and chemically (etched). Surface orientation was controlled by a standard method. The "Rigaku Denki" A-3 camera has been used in the experiments. A divergent beam has been used, which made it possible to simultaneously register the multibeam region and the two-beam background on the same topograph. The incident beam front was limited by a narrow slit having 0.2 mm width.

All three cases shown in Fig. 1 have been analysed. Under diffraction of radiation in the first case, when only one (044) beam is Bragg reflected, the angle α between the crystal surface and the $(1\bar{1}1)$ plane is equal to 55°. In the second case $\alpha = 90°$ (the crystal surface is parallel to the (011) plane). Here three beams emerge from the crystal through the input surface, making the same angles with the surface as do the Laue-diffracted beams. The third case is the opposite of the first: the incident beam forms a 15° angle with the surface, which is equal to the angle between the (044) beam and the surface in the first case ($\alpha = 125°$). Since in the third case, the incident beam enters the crystal almost parallel to its surface, samples of thickness not larger than 380 mm have been investigated.

The experimental results may be summarized as follows. In the first and second cases on the Laue topographs ((000), (220) $(\bar{2}02)$, (242), and $(\bar{2}24)$ in the first case, and on (000), (220), and $(\bar{2}02)$ in the second case) the multibeam region is weakly visible against the background of two-beam lines, though the two-beam lines themselves are distinctly visible. Thus the anomalous transmission enhancement effect in these cases is almost unobservable experimentally, which agrees with results of experiments, where the pure Laue-geometry case has been considered [4, 8, 11]. In these cases the two-beam bands are sufficiently intensive, since they are formed as a result of two-beam Laue diffraction. In the third case the multi-beam region on the transmission beam topographs is distinctly visible as a region of enhanced intensity against the background of (220) and $(\bar{2}02)$ lines (see Fig. 2). Two-beam lines in this case originate as a result of the Borrmann effect in the process of two-beam Bragg diffraction and these lines are weaker than in the Laue case. Therefore, the multibeam enhancement of intensity appears to be more visible. One should remember that in the given experimental set-up the image on the topograph is strongly averaged and broadened because of the non-monochromatic character of the incident radiation within the limits of intrinsic linewidth [14].

For the Bragg-reflected beams the most interesting features have been observed on the (044)-beam topographs (see Fig. 3). Indeed, in the first and third cases the multibeam region on the (044)-beam topograph appears as a dark narrow strip on the background of a light vertical band corresponding to two-beam scattering (Fig. 3 a and c). The two-beam band is strongly broadened in the transverse direction due to the non-monochromatic character of radiation, the result of which is a non-symmetric form of the multibeam region. The actual dimensions of the multibeam region coincide with

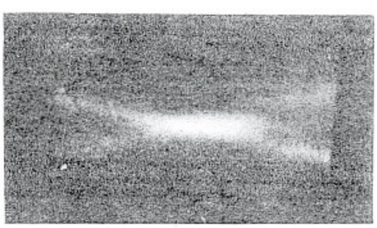

Fig. 2. (000) beam experimental topograph in the third case

the dark horizontal strip width. In the second case, on the contrary, the multibeam region appears to be lighter than the two-beam line background (Fig. 3b).

The decrease of intensity for the Bragg-reflected beam in multibeam scattering is obvious from the physical point of view. In the two-beam case practically all the energy of the incident plane wave is reflected into the diffracted beam in the maximum reflection region. In the multibeam scattering a part of the intensity is transferred to the other diffracted beams, hence the intensity of the given beam is reduced. This effect has

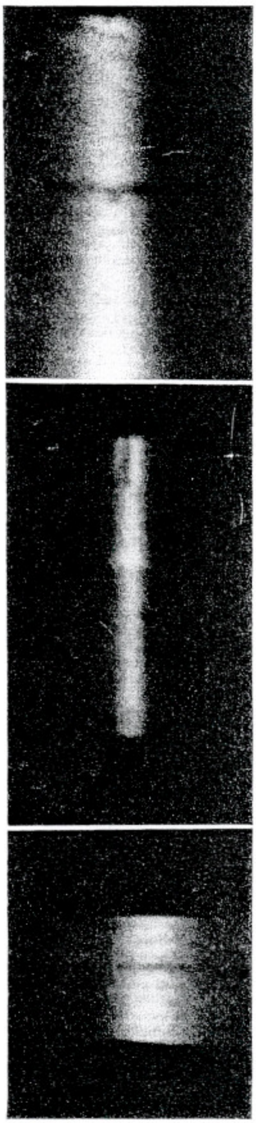

a

b

c

Fig. 3

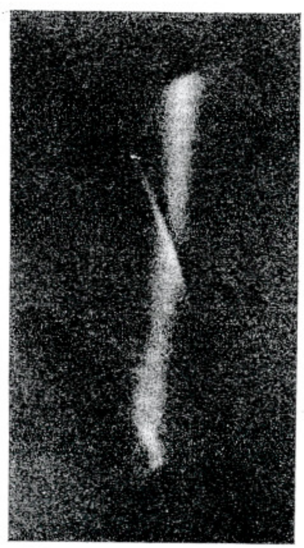

Fig. 4

Fig. 3. (044) reflex in a) the first case, b) the second case, c) the third case

Fig. 4. (242) reflex in the third case

been discovered as early as in 1928 by Meyer [15] in the case of three-beam scattering and has been named the "aufhellung" effect. However, the increase of intensity, i.e. the two-beam Bragg reflection enhancement due to multi-beam scattering in the second case, has been observed for the first time. We will return to this effect in the next section.

The multibeam region on the topograph of Bragg reflections (242) and ($\bar{2}24$) in the second and third cases has a fine structure, i.e. there is an alternation of enhanced and reduced intensity regions. Diffraction pattern broadening due to non-monochromaticity takes place in the S-plane inclined at a certain angle to a two-beam band [14]. This is clearly visible in Fig. 4, where the (242) beam topograph in the third case is shown. The multibeam enhancement area is broadened more than the two-beam band. Due to the non-monochromatic character of the radiation in the centre of the two-beam band, and integral intensity along the intersection of S-plane and topograph plane is actually being measured.

The above-described results have been obtained for CuK_α radiation. Similar experiments have been carried out with MoK_α radiation. In the latter case we could observe only the intensity enhancement in the direct beam. The six-beam area on topographs of all diffracted beams was undistinguishable from the two-beam background. This fact is probably due to poor resolution of the experiment. With decrease of wavelength the multibeam area is narrowed and no longer resolved on diffraction topographs.

3. Theory and Discussion of Results

To understand the mechanism of the X-ray interaction with the crystal in the process of multibeam sacttering one has to know the spatial structure of the standing X-ray wave forms, originated in the process of plane-wave diffraction, as well as the angular dependence of the interference absorption coefficients and of intensities for the incident and diffracted beams. A useful method for the numerical evaluation of these characteristics has been suggested in [13].

The problem was shown to reduce to an eigenvalue problem for a twelfth-order complex scattering matrix, and the solution of a twelfth-order system of linear, inhomogeneous equations in order to obtain the excitation degree for various regions of the dispersion surface from the boundary conditions.

The scattering amplitude of the incident plane wave in polarization state s' into the m-th diffracted wave in polarization state $s(s, s' = \pi, \sigma)$ is represented in the following form [13]:

$$P_m^{ss'}(t) = \sum_j B_{ms}(j)\, \lambda_{s'}(j, t)\, D_m(j, t)\,, \tag{1}$$

where

$$D_m(j, t) = \begin{cases} \exp\,(i\varepsilon_j t/2)\,; & \gamma_m > 0\,, \\ 1\,; & \gamma_m < 0\,. \end{cases} \tag{2}$$

In these expressions ε_j and $B_{ms}(j)$ are eigenvalues and normalized eigenvectors of the scattering matrix, respectively, $\lambda_s(j, t)$ is the excitation value of the j-th mode depending on the crystal thickness t, γ_m is the direction cosine of the m-th wave vector with respect to the inward normal $\boldsymbol{n}$ to the crystal surface.

The incident wave vector $\boldsymbol{k}_0$ may be expressed in the vicinity of the multi-wave scattering direction in the following form:

$$\boldsymbol{k}_0 = \boldsymbol{\varkappa}_0 + \frac{2\pi}{\lambda}\,(\theta_1 \boldsymbol{n}_R + \theta_2 \boldsymbol{e}_{0\sigma} + \theta_3 \boldsymbol{n}_h)\,, \tag{3}$$

where $\varkappa_0$ is a vector that strictly satisfies all multi-wave diffraction conditions $(\varkappa_0 + h_m)^2 = \varkappa_0^2$ for the frequency ω_0 corresponding to maximum intensity in the radiation spectrum, h_m are reciprocal lattice vectors, λ is the radiation wavelength. In the case considered all reciprocal lattice vectors lie in the same plane (H-plane), n_h is the unit vector normal to this plane, and n_R is the unit vector along the direction that connects the centre of the circle circumscribing the reciprocal lattice vector hexads with the point O, $e_{0\sigma} = [n_h \times n_R]$. Parameters θ_1, θ_2, and θ_3 describe small deviations of vector k_0 from $\varkappa_0$ both in direction and magnitude. Clearly, the IAC (imaginary part of ε_j) as well as the transmission and reflection coefficients do not depend on θ_3. While the parameter θ_2 completely determines the direction of the vector k_0, variations of the parameter θ_1 may arise from changes in the direction of the incident wave vector in a plane determined by vectors n_h and $\varkappa_0$ (S-plane) as well as due to radiation wavelength variations.

The excitation values $\lambda_s(j, t)$ in the general case have a complex and non-analytic dependence on the crystal thickness. Also, in a set of $2N$ eigenvalues $\varepsilon_j (N = 6)$ there exist elements with negative imaginary part $(\varepsilon_j'' < 0)$. The number of such elements is equal to $2M$ where M is the number of Bragg-reflected beams. Waves corresponding to such regions have amplitudes increasing with increasing crystal thickness. They describe the X-ray reflection from the lower output surface of the crystal. Excitation values for such waves obviously fall off abruptly with increasing crystal thickness. However, the numerical verification of this result is rather difficult, since the matrix of a linear inhomogeneous system of equations turns out to be weakly defined: when $t \gg L_A$, where L_A is the absorption length, the matrix contains anomalously large numbers. In the limiting case when $t \to \infty$ one may use the approximation $\lambda_s(j, \infty) = 0$, if $\varepsilon_j'' < 0$ [13, 16]. The remaining excitation values are then obtained from a truncated system of equations, corresponding to boundary conditions only on the input crystal surface.

Such an approximation turns out to be sufficient for the evaluation of Bragg reflection coefficients, which are independent of the crystal thickness when $t \to \infty$. On the other hand, in this case transmission and reflection coefficients for the Laue beams depend on thickness. For their evaluation it is convenient to represent the reflection and transmission coefficients in the form of a power series of a small parameter $\exp(-t/L_A)$. The first terms of this series have the following form:

$$P_m^{ss'}(t) = \sum_j e^{i\varepsilon_j t/2} \left[B_{ms}^j - \sum_{i,ks''} B_{ms}^i \beta_i^{ks''} B_{ks''}^j\right] \alpha_j^{0s'} , \tag{4}$$

$$P_k^{ss'} = \sum_j B_{ks}^j \alpha_j^{0s'} . \tag{5}$$

In these formulae the index j numerates only the eigenvalues ε_j with positive imaginary parts $(\varepsilon_j'' > 0)$ and index i those with negative imaginary parts $(\varepsilon_i'' < 0)$, the index m numerates Laue beams, including the incident beam $(\gamma_m > 0)$, and the index k denotes Bragg-reflected beams $(\gamma_k < 0)$. Accordingly the eigenvector matrix $\hat{B}$ is divided into four blocks: two square blocks along the diagonal and two rectangular off-diagonal blocks. Matrices $\hat{\alpha}$ and $\hat{\beta}$ are inverse matrices of square blocks,

$$\sum_{ms} \alpha_{j'}^{ms} B_{ms}^j = \delta_{jj'} , \qquad \sum_{ks} \beta_{i'}^{ks} B_{ks}^i = \delta_{ii'} . \tag{6}$$

Expression (4) is convenient also in the sense that it allows to carry out in explicit form the smoothening of small oscillations in the Laue beam intensities, corresponding to interband interactions. While the reflection coefficient for the Bragg beams has its usual form,

$$R_k(\theta_1, \theta_2) = \tfrac{1}{2} \sum_{ss'} |P_k^{ss'}|^2 , \tag{7}$$

for the Laue beams this coefficient is approximately equal to

$$R_m(\theta_1, \theta_2, t) = \tfrac{1}{2} \sum_{ss'} \sum_j \mathrm{e}^{-\mu_j t} \, |(B^j_{ms} - \sum_{i,\,ks''} B^i_{ms} \beta^{ks''}_i B^j_{ks'}) \, \alpha^{0s'}_i|^2 \, , \tag{8}$$

where $\mu_j = \varepsilon''_j$ are interference absorption coefficients. Formulae (7) and (8) are basic for further calculations.

Table 1

α	$\mu_{\min}$ (cm^{-1})	μ_0/γ_0 (cm^{-1})
$-30°$	1.13	2145
$-20°$	1.16	1060
$-10°$	1.24	719
0°	1.40	557
10°	1.24	466
20°	1.16	411
30°	1.13	378
40°	1.12	360
50°	1.15	354
60°	1.22	359
70°	1.35	376
80°	1.55	407
90°	1.91	459
100°	2.53	545
110°	3.99	697
120°	16.28	1011

Calculations have been carried out under the same geometrical conditions as the experimental observation (see Fig. 1). Fig. 5 shows the reciprocal lattice vectors and the two-beam line structure in the plane of parameters θ_1 and θ_2. Transmission and reflection coefficients have been evaluated for crystals of thickness 200, 100, and 50 μm in the first, second, and third cases, respectively (Fig. 1). Calculations have shown that a strong decrease of multi-beam minimal IAC takes place in a broad range of angles formed by the crystal surface and the plane of reciprocal lattice vectors. This result follows from the data of Table 1, where together with the minimal IAC the values of the linear absorption coefficient in the one-beam case in the direction normal to the surface are given. It also follows from Table 1 that in the symmetrical Laue case ($\alpha = 0$) the minimum IAC value along the normal to the surface is slightly higher than the absolute minimum corresponding to $\alpha = 40°$, when the reflected (044) beam is

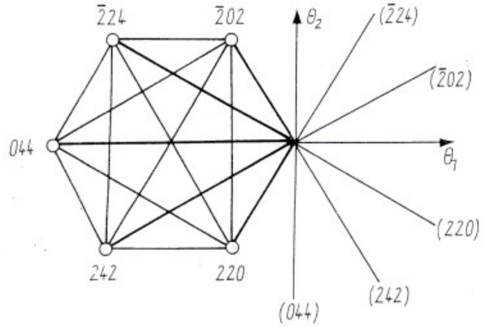

Fig. 5. Reciprocal lattice vectors and two-beam line structure

parallel to the crystal surface and the incident beam forms an angle of 80° with this surface. In the general case of non-symmetric diffraction ($\alpha \neq 0$) the minimum value of IAC is attained under certain reflection of the incident wave vector from the exact multibeam direction. At the point of the minimum the angle θ_2 is equal to zero, however $\theta_1 \neq 0$ has the sign of α and increases with the magnitude of α.

Now, what is the mechanism of anomalous transmission enhancement? To answer this question lets consider the dependence of IAC on the wave amplitudes. It was shown in [17] that the following relation is valid:

$$\mu_j = \mu_0 S_z^{-1}(j) \sum_{mm'} \boldsymbol{E}_m^*(j) \frac{\chi_{imm'}}{\chi_{i0}} \boldsymbol{E}_{m'}(j) , \tag{9}$$

where $\boldsymbol{E}_m(j)$ is the electrical field amplitude of the m-th wave, corresponding to the j-th region of the dispersion surface $S_z(j)$, z is the component (normal to the surface) of the energy flux vector from the j-th region,

$$\boldsymbol{E}_m(j) = \sqrt{\gamma_m} \sum_s B_{ms}(j) \, \boldsymbol{e}_{ms} , \tag{10}$$

$$S_z(j) = \sum_m |\boldsymbol{E}_m(j)|^2 \gamma_m , \tag{11}$$

$\mu_0 = (2\pi/\lambda) \chi_{i0}$ is the normal absorption coefficient, $\boldsymbol{e}_{ms}$ the polarization vector, $\chi_{imm'}$ the Fourier component of the imaginary part of the crystal polarizability χ_i for a reciprocal lattice vector $(\boldsymbol{h}_m - \boldsymbol{h}_{m'})$. The quantity χ_i is generally a tensor, however, in the dipole approximation giving the main contribution to absorption, this quantity has a simple scalar structure. Here the ratio $\chi_{imm'}/\chi_{i0}$ is simply equal to the Debye-Waller factor.

With an account of the arguments given above one may easily see that the double sum in (9) represents the resulting field intensity of the j-th region in sites of the crystal lattice, averaged over the thermal vibrations of the atoms,

$$\mu_j \approx \mu_0 S_z^{-1}(j) \langle I_j(\boldsymbol{R}_n + \boldsymbol{U}_n) \rangle , \tag{12}$$

where $\boldsymbol{R}_n$ and $\boldsymbol{U}_n$ are equilibrium position and displacement vectors, respectively,

$$I_j(\boldsymbol{r}) = |\sum_m \boldsymbol{E}_m(j) \exp (i\boldsymbol{h}_m \boldsymbol{r})|^2 . \tag{13}$$

The function $I_j(\boldsymbol{r})$, according to its definition, describes a two-dimensional standing wave in the H-plane with a period which is a multiple of the crystal lattice period. Numerical evaluation of this function shows that the IAC decreases, since at certain incident angles of the plane wave standing waves originate with nodes located exactly in the sites of a two-dimensional lattice, representing the lattice projection on the H-plane. An example of such a standing wave is given in Fig. 6, where the level curves

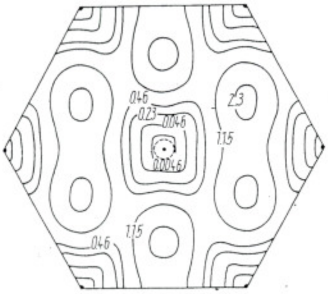

Fig. 6. Intensity of the interatomic X-ray field standing wave in the crystal region with minimum absorption coefficient in the second case. Atomic projections are located in the centre and the vertices of a hexagon

of given values of function $I_j(\boldsymbol{r})$ normalized by its mean value are shown, for the field with minimum absorption coefficient $\mu_j = 1.91\ \text{cm}^{-1}$ and the following values of the parameters: $\theta_1 = 0.65''$, $\theta_2 = 0$, $\alpha = 90°$. The dotted circle limits the cross-section of the atomic nucleus under thermal vibrations.

The angular dependence of the transmission and reflection coefficients in the second of the considered cases ($\alpha = 90°$, $t = 100\ \mu\text{m}$) is shown in Fig. 7 a to d. One may easily observe an increase of intensity in the multibeam range of angles both for the transmitted beam and for the Laue-diffracted (220) beam. However, the transmission coefficient is significantly larger than the reflection coefficient. The intensity of the Bragg-reflected (242) and (044) beams is decreased in the multibeam range of the "aufhellung" angles, however, one may note a local increase of intensity on the (044) beam pattern near the Bragg direction. Such intensity increase is absent on the angular dependence diagrams for the (044) beam in the first and third cases of Fig. 1.

For all diffracted beams a clearly defined enhancement in directions of other diffracted beams is observed, which is due to indirect interactions of these beams. Obviously, this effect is most definitely expressed in the range of angles where the direct interaction with the incident beam is weak, while the interaction of the incident beam with the other reflected beam and interaction of reflected beams with each other is still strong, i.e. when corresponding Bragg conditions hold.

In order to compare our theory with the experiment we have calculated the integral intensity over angle θ_1 for the (044) beam in all three cases. The results of this calcula-

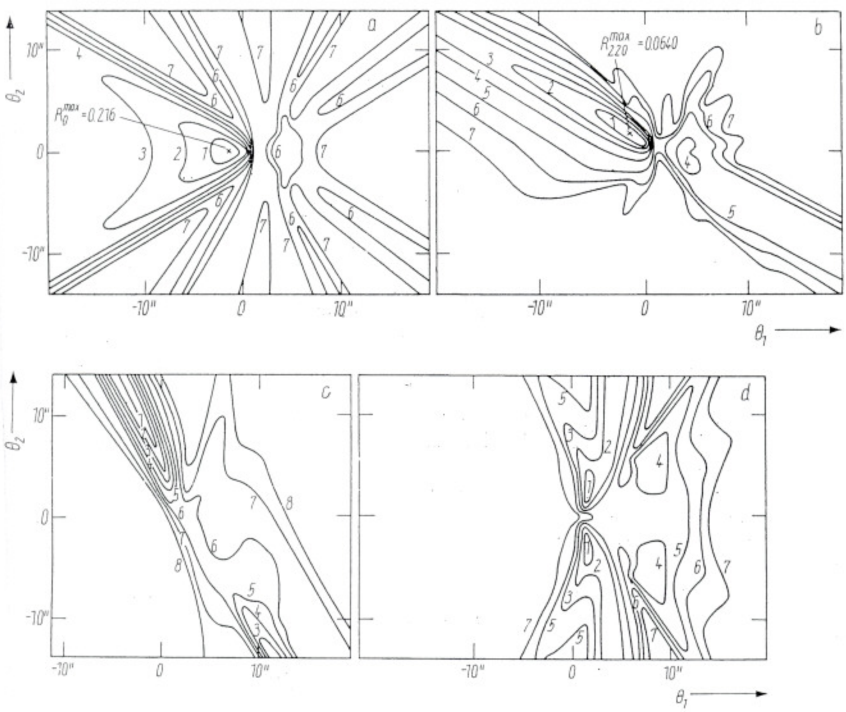

ig. 7. Angular dependence of a) (000) beam ($R_0/R_0^{\max}$=0.9 (1), 0.7 (2), 0.5 (3), 0.3 (4), 0.2 (5) 0.1 (6), 05 (7), b) (220) beam ($R_{220}/R_{220}^{\max} = 0.8$ (1), 0.6 (2), 0.4 (3), 0.2 (4), 0.08 (5), 0.04 (6), 0.02 (7)), (242) beam ($R_{102} = 0.565$ (1), 0.424 (2), 0.353 (3), 0.282 (4), 0.212 (5), 0.141 (6), 0.071 (7), 035 (8)), d) (044) beam ($R_{044} = 0.441$ (1), 0.331 (2), 0.220 (3), 0.165 (4), 0.110 (5), 0.055 (6), 028 (7)) in the second case

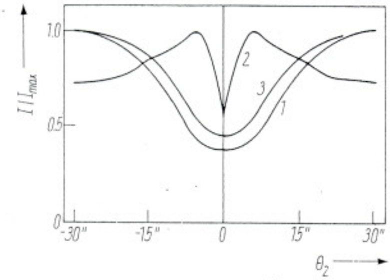

Fig. 8. Theoretical intensity of a (044) beam integrated over angle θ_1 in the first (curve 1), second (curve 2), and third (curve 3) case

tion, normalized to maximum value, are shown in Fig. 8. One may observe from this figure that the anomalous behaviour of a multi-beam region for the (044) beam in the second case, which has been observed experimentally, is in qualitative agreement with the theory. A narrow gap in the central part of curve 2, shown in Fig. 8, is invisible on the experimental topograph due to poor resolution, however, one could notice this gap on the negative plate.

The anomalous increase of intensity for the (044) beam in six-beam scattering is apparently related to an indirect excitation effect, which is similar to the Renninger effect [18]. Indeed, the Bragg angle for the (044) reflection is equal to $\theta_B^{(044)} = 50.5°$, therefore the polarization factor for the π-polarization, being equal to $\cos 2\theta_B = 0.19$, is close to zero. As a result of this practically only half of the radiation is reflected in the two-beam case, namely the one corresponding to σ-polarization. In the process of multi-beam scattering an additional reflection of the π-polarized radiation is possible due to indirect interaction via the other reflections. This results in an increase of the reflection coefficient.

Thus, the results of our investigation show that the six-beam X-ray diffraction in the case of a mixed Bragg–Laue geometry represents an interesting and practically important phenomenon. The existence of strong enhancement for anomalous transmission of the Laue beams, together with strong Bragg reflection of radiation, makes it possible to create new types of monochromators and interferometers.

References

[1] T. Joko and A. Fukuhara, J. Phys. Soc. Japan **22**, 597 (1967).
[2] M. Umeno, phys. stat. sol. (a) **2**, K203 (1970).
[3] M. Umeno, phys. stat. sol. (a) **11**, 501 (1972).
[4] T. C. Huang, H. H. Tillinger, and B. Post, Z. Naturf. **28a**, 600 (1973).
[5] M. Umeno, phys. stat. sol. (a) **37**, 561 (1976).
[6] M. Umeno, phys. stat. sol. (a) **38** 701 (1976).
[7] V. G. Kohn, Fiz. tverd. Tela **18**, 2538 (1976).
[8] S. A. Kshevetskii and I. P. Mihalyuk, Kristallografiya **21**, 381 (1976).
[9] A. M. Afanasev and V. G. Kohn, Acta cryst. **A33**, 178 (1976).
[10] I. P. Mikhailyuk, S. A. Kshevetskii, V. D. Kozmik, and M. V. Ostapovich, Kristallografiya **23**, 399 (1978).
[11] I. P. Mikhailyuk, S. A. Kshevetskii, M. V. Ostapovich, and V. D. Kozmik, Kristallografiya **23**, 403 (1978).
[12] S.-L. Chang, Z. Naturf. **37a**, 501 (1982).
[13] V. G. Kohn, phys. stat. sol. (a) **54**, 375 (1979).
[14] V. G. Kohn, Fiz. tverd. Tela **19**, 3567 (1977).
[15] G. Z. Meyer, Krist. **66**, 585 (1928).
[16] S.-L. Chang, Acta cryst. **A35**, 543 (1979).
[17] A. M. Afanasev and V. G. Kohn, phys. stat. sol. (a) **28**, 61 (1975).
[18] M. Renninger, Z. Krist. **97**, 107 (1937).

(Received January 23, 1984)